Electrical excitation of shock and solitonlike waves in two-dimensional electron channels

E. Vostrikova and A. Ivanov
Department of General Physics, Moscow Institute of Physics and Technology, Dolgoprudny 141700, Russia

I. Semenikhin and V. Ryzhii*
Computer Solid State Physics Laboratory, University of Aizu, Aizu-Wakamatsu 965-8580, Japan
(Received 4 April 2007; revised manuscript received 16 May 2007; published 2 July 2007)

We study the electrical excitation of nonlinear plasma waves in heterostructures with two-dimensional electron channels and with split gates, and the propagation of these waves using hydrodynamic equations for electron transport coupled with two-dimensional Poisson equation for self-consistent electric potential. The term related to electron collisions with impurities and phonons as well as the term associated with viscosity are included into the hydrodynamic equations. We demonstrate the formation of shock and solitonlike waves as a result of the evolution of a strongly nonuniform initial electron density distribution. It is shown that the shock wave front and the shape of solitonlike pulses pronouncedly depend on the coefficient of viscosity, the thickness of the gate layer, and the nonuniformity of the donor distribution along the channel. The electron collisions result in the damping of the shock and solitonlike waves, while they do not markedly affect the thickness of the shock wave front.

DOI: 10.1103/PhysRevB.76.035401 PACS number(s): 73.21.−b, 73.40.−c, 73.43.Lp, 73.43.Cd

I. INTRODUCTION

Plasma waves, i.e., self-consistent spatiotemporal variations of the electron density and electric field in two-dimensional electron gas (2DEG) channels[1–5] can be used in different semiconductor heterostructure devices. One of the most important advantages of 2DEG systems in comparison with three-dimensional electron gas systems is the possibility of realizing situations when the characteristic plasma frequency markedly exceeds the frequency of electron collisions with impurities and phonons. This is achieved using the selective doping when donors are spatially separated from the 2DEG channel, so that the electron density can be rather high, while the electron-impurity interaction is weakened. In 2DEG systems with highly conducting electrodes (gates) similar to field-effect transistor structures, the electron density can be effectively controlled (in particular, significantly increased) by the applied voltage. Another attractive feature of the 2DEG system is that at realistic parameters, the characteristic plasma frequency falls in the terahertz range. This opens up the prospects of creating novel terahertz devices, for example, sources and detectors of terahertz radiation, frequency multipliers, and so on.[6–8] In recent experiments,[9–16] the detection of terahertz radiation in and terahertz emission from transistorlike 2DEG systems associated with the resonant excitation of plasma waves was realized (see also Refs. 17–20). Results of theoretical studies of plasma phenomena in 2DEG systems have been reported in numerous publications. However, nonlinear plasma phenomena in these systems are studied far less extensively. In particular, the plasma phenomena associated with hydrodynamic nonlinearities in 2DEG transport were considered in Refs. 21–27. The effect of nonlinearities associated with different contact effects were considered theoretically in Refs. 28–30. Nevertheless, nonlinear properties of 2DEG systems can themselves be used in device applications. This and the recent progress in experimental studies of terahertz plasma phenomena stimulate a significant interest in nonlinear plasma effects in different 2DEG systems.

In this paper, we study nonlinear plasma phenomena associated with the electrical excitation of plasma waves in 2DEG systems using both analytical treatment and numerical modeling. We consider structures with a 2DEG channel supplied with side contacts and a system of highly conducting electrodes (split gates), which provides an opportunity to control the 2DEG by applying voltage signals. The structures under consideration are schematically shown in Fig. 1. We use the hydrodynamic model for electron transport along the channel coupled with the 2D Poisson equation for self-consistent electric potential in and around the channel. In

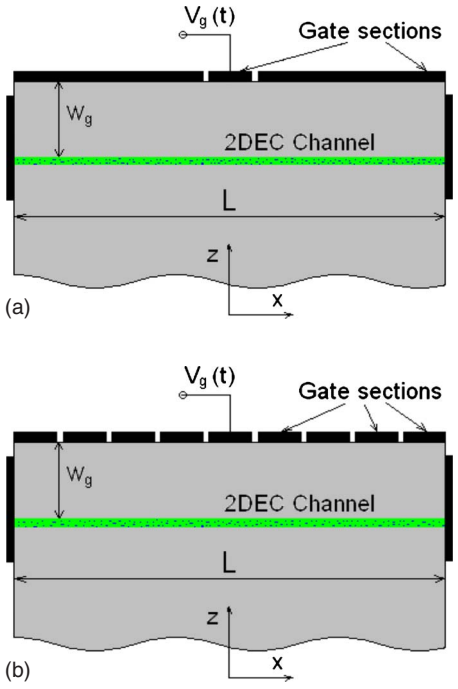

FIG. 1. (Color online) Schematic view of heterostructures with a 2DEG channel and with split gate electrode configurations.

contrast to previous studies of nonlinear waves in 2DEG systems,[21–25] we take into consideration the 2D nature of the potential distributions. This allows us to follow the change in nonlinear wave properties with the transition from 2DEG systems with the gates very close to the channel to those with rather remote gates when the plasmon spectrum essentially varies. The effect of spacing between 2DEG and highly conducting gates on the linear plasma properties was studied through many papers beginning with the paper by Chaplik.[2] (See, in particular, Refs. 31–34, where the role of the gates and contacts on the spectra of linear plasma oscillation was considered.)

As one might expect and is shown below, the 2DEG systems with different plasmon spectra exhibit different behaviors for nonlinear plasma waves. This is akin to the difference in properties of gravity surface waves in shallow and deep water pools.[6,7,22,35] Apart from this, in our numerical modeling, we focus on electron scattering on impurities and phonons as well as on the 2DEG viscosity due to electron-electron collisions.

II. EQUATIONS OF THE MODEL

We consider the hydrodynamic equations (the Navier-Stokes equation and the continuity equation) and the Poisson equation in the following form:

$$\frac{\partial v}{\partial t} + \nu v \frac{\partial v}{\partial x} - K\frac{\partial^2 v}{\partial x^2} = \frac{e}{m}\frac{\partial \varphi}{\partial x}, \tag{1}$$

$$\frac{\partial \Sigma}{\partial t} + \frac{\partial \Sigma v}{\partial x} = 0, \tag{2}$$

$$\frac{\partial^2 \psi}{\partial x^2} + \frac{\partial^2 \psi}{\partial z^2} = \frac{4\pi e}{æ}(\Sigma - \Sigma_d)\delta(z). \tag{3}$$

Here, $v=v(t,x)$ and $\Sigma=\Sigma(t,x)$ are the electron hydrodynamic velocity along and sheet density in the 2DEG channel, $\psi=\psi(t,x,z)$ is the electric potential, $\varphi=\psi(t,x,0)$ is the electric potential in the channel ($z=0$), $\Sigma_d=\Sigma_d(x)$ is the donor sheet concentration in the 2DEG channel (or near it), ν is the frequency of the electron scattering on impurities and phonons, K is the coefficient of viscosity associated with the electron-electron scattering processes, $e=|e|$ and m are the electron charge and effective mass, respectively, $æ$ is the dielectric constant, and $\delta(z)$ is the Dirac delta function describing the electron confinement in a relatively narrow channel (its width is assumed to be much smaller than any lateral size and the distance between the 2DEG channel and the gate electrode). The axis x is directed along the channel, so that the coordinates of the side contacts are $x=\pm L/2 \simeq \pm L_g/2$, where L and L_g are the lengths of the channel and gate (see Fig. 1), respectively ($L_g \leq L$). The axis z is directed perpendicular to the 2DEG channel. The latter corresponds to $z=0$, whereas the gate electrode corresponds to $z=W_g$, where W_g is the thickness of the gate layer. In Eq. (1), we disregard the term corresponding to the gradient of the pressure in 2DEG in comparison with the electric force (see, for instance, Ref. 25). The boundary conditions follow from the assumption that the electron sheet densities at the side contacts are fixed and that the electric potentials at the electrodes (the side contacts to the channel and the gate sections) are given functions of time. For the electric potential at nonconducting surfaces (between the electrodes), linear approximation is used. It is also assumed that at $z \to -\infty$, the electric field $\partial\psi/\partial z \to 0$. The equations of the model under consideration account for the generally two-dimensional character of the potential spatial distribution, as well as the electron transport in the 2DEG channel considering electron scattering and viscosity.

In the case of the structures with a relatively small thickness of the gate layer W_g ($W_g \ll \lambda$, where λ is the characteristic length of the electron density and electric potential nonuniformities), the Poisson equation [Eq. (3)] can be replaced by the following:

$$\frac{\varphi - V_g}{W_g} = \frac{4\pi e}{æ}(\Sigma_d - \Sigma). \tag{4}$$

We shall consider the following case. It is assumed that generally the bias dc voltage V_g is applied to the side gate sections. Apart from this, a relatively high transient voltage $V_g(t)$ is applied to the central section, so that $V_g(t)=V_g+\Delta V_g[\Theta(-t)+\Theta(t)\exp(-t/t_0)]$, where $\Theta(t)$ is the unity step function and t_0 is the characteristic time of the gate section recharging. The recharging time t_0 is determined by the capacitance C_0 of the gate section and the pertinent resistance R_0 of the control circuit: $t_0=R_0C_0$. The bias gate voltages result in a nonuniform distribution of the electron density along the channel, which at $t<0$ exhibits a maximum in the channel center. We shall mainly consider 2DEG systems with uniformly distributed donors in the channel (or in the gate layer slightly above the channel). The case of strongly nonuniform doping along the channel will be briefly studied as well (in Sec. V).

The linearized version of Eqs. (1)–(3) governs the propagation of the plasma waves with the dispersion relation, which in the case V_g=const is given by the following formula:

$$\omega[\omega + i(\nu + Kq^2)] = \frac{s_0^2 q}{W_g[\coth(|q|W_g) + 1]}. \tag{5}$$

Here, ω and q are the frequency and wave number of a linear plasma wave,

$$s_0 = \sqrt{\frac{4\pi e^2 \Sigma_0 W_g}{æm}} \tag{6}$$

is the characteristic velocity of the plasma wave in the gated 2DEG channel, and

$$\Sigma_0 = \Sigma_d + \frac{æ V_g}{4\pi e W_g} \tag{7}$$

is the ac electron sheet density. In the limits of long waves ($qW_g \ll 1$) and short waves ($qW_g \gg 1$), Eq. (5) yields the following relationships:[1,3]

$$\mathrm{Re}\ \omega \simeq s_0 q\left(1-\frac{|q|W_g}{2}\right) \tag{8}$$

and

$$\mathrm{Re}\ \omega \simeq s_0\sqrt{\frac{|q|}{2W_g}}. \tag{9}$$

The dispersion relations given by Eqs. (5), (8), and (9) are similar to those for gravity waves on the surface of a water channel. In particular, Eq. (8) corresponds to the so-called "shallow water" case, whereas Eq. (9) corresponds to the "deep water" case (see, for instance, Refs. 6, 7, 22, and 35). This is a consequence of the analogy of Eqs. (1)–(3) and the pertinent hydrodynamic equations for waves on the surface of a liquid under gravity force. The damping rate of the plasma wave (in the case $\nu+Kq^2 \ll \mathrm{Re}\ \omega$) is given by

$$\mathrm{Im}\ \omega \simeq -\frac{1}{2}(\nu+Kq^2). \tag{10}$$

III. RIEMANN SOLUTION AND SHOCK WAVE FORMATION

Consider first Eqs. (1), (2), and (4). Assuming that the gate layer is sufficiently thin, the length of the channel is sufficiently large, so that we may disregard the boundary conditions, and that the electron collisions with impurities and phonons as well as the viscosity can be neglected. In this case, we arrive at the following equations:

$$\frac{\partial v}{\partial t}+v\frac{\partial v}{\partial x}=\frac{e}{m}\frac{\partial \varphi}{\partial x}, \tag{11}$$

$$\frac{\partial \Sigma}{\partial t}+\Sigma\frac{\partial v}{\partial x}=-v\frac{\partial \Sigma}{\partial x}, \tag{12}$$

$$\frac{e\varphi}{m}=s_0^2\left(1-\frac{\Sigma}{\Sigma_0}\right). \tag{13}$$

The system of Eqs. (11)–(13) can be presented as

$$\frac{\partial v}{\partial t}+v\frac{\partial v}{\partial x}=-\frac{s_0^2}{\Sigma_0}\frac{\partial \Sigma}{\partial x}, \tag{14}$$

$$\frac{\partial \Sigma}{\partial t}+\Sigma\frac{\partial v}{\partial x}=-v\frac{\partial \Sigma}{\partial x}. \tag{15}$$

As pointed out above, Eqs. (14) and (15) are akin to the equations governing gravity waves in shallow water channels. They are also identical in form to the equations governing isentropic flows of a compressible gas with the adiabatic index $\gamma=2$. This indicates that Eqs. (14) and (15) have solutions in the form of the Riemann waves which, under certain conditions, can transform into shock waves.[35,36] One also needs to point out that the solution of Eqs. (14) and (15) should describe nonlinear waves, with the front steepening with time until the moment when the solution becomes three valued. Analyzing Eqs. (14) and (15), we shall use a standard approach (see, for instance, Refs. 36 and 37), assuming that $v=v(\Sigma)$. Considering the latter, Eqs. (14) and (15) become as follows:

$$\frac{dv(\Sigma)}{d\Sigma}\left[\frac{\partial \Sigma}{\partial t}+v(\Sigma)\frac{\partial \Sigma}{\partial x}\right]=-\frac{s_0^2}{\Sigma_0}\frac{\partial \Sigma}{\partial x}, \tag{16}$$

$$\frac{\partial \Sigma}{\partial t}+v(\Sigma)\frac{\partial \Sigma}{\partial x}=-\Sigma\frac{dv(\Sigma)}{d\Sigma}\frac{\partial \Sigma}{\partial x}. \tag{17}$$

Equations (16) and (17) are identical if

$$\Sigma\left[\frac{dv(\Sigma)}{d\Sigma}\right]^2=\frac{s_0^2}{\Sigma_0}. \tag{18}$$

Equation (18) results in

$$\frac{dv(\Sigma)}{d\Sigma}=\pm\frac{s_0}{\sqrt{\Sigma_0\Sigma}}. \tag{19}$$

Considering the solution corresponding to the sign "+" in Eq. (19) and introducing

$$s=s_0\sqrt{\frac{\Sigma}{\Sigma_0}}, \tag{20}$$

we obtain

$$v(\Sigma)=2s+\mathrm{const}. \tag{21}$$

Assuming that $\Sigma=\Sigma_0$ at $v=0$, we find

$$v(\Sigma)=2(s-s_0)=2s_0\left(\sqrt{\frac{\Sigma}{\Sigma_0}}-1\right). \tag{22}$$

Using Eq. (22) with Eqs. (16) and (19), we arrive at the Riemann solution,

$$x=[v(\Sigma)+s(\Sigma)]t+C(\Sigma), \tag{23}$$

where $s(\Sigma)$ is given by Eq. (20) and $C(\Sigma)$ is determined by the initial conditions. Hence, the electron density as a function of x and t is given (in implicit form) by the following equation:

$$x=s_0\left(3\sqrt{\frac{\Sigma}{\Sigma_0}}-2\right)t+C(\Sigma). \tag{24}$$

Using Eq. (24), we can find the wave breaking time t_{br}, i.e., the time of formation of the discontinuity or the time of formation of a shock wave. This time is determined by the following conditions:[35]

$$\left.\frac{\partial x}{\partial \Sigma}\right|_{t=t_{br}}=0, \qquad \left.\frac{\partial^2 x}{\partial \Sigma^2}\right|_{t=t_{br}}=0. \tag{25}$$

Equations (25) yield

$$t_{br}=-\frac{2}{3}\frac{\sqrt{\Sigma_0\Sigma}}{s_0}\left.\frac{dC(\Sigma)}{d\Sigma}\right|_{t=t_{br}} \tag{26}$$

and

$$t_{br}=\frac{4}{3}\frac{\Sigma_0^{1/2}\Sigma^{3/2}}{s_0}\left.\frac{d^2C(\Sigma)}{d\Sigma^2}\right|_{t=t_{br}}. \tag{27}$$

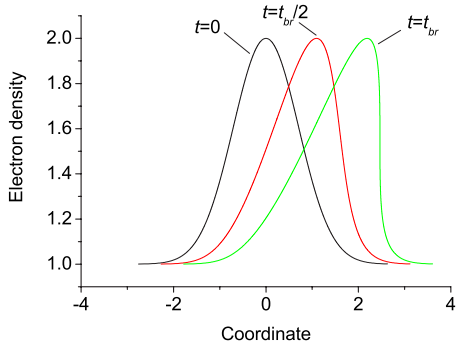

FIG. 2. (Color online) Transformation of the spatial distribution of the normalized electron density Σ/Σ_0 in the Riemann wave governed by Eq. (23) with the initial condition in Eq. (28) and $\Delta\Sigma_0/\Sigma_0=1$.

As an example, let us consider the case when the initial distribution of the electron density is as follows:

$$\Sigma|_{t=0} = \Sigma_0 + \Delta\Sigma_0 \exp\left[-\left(\frac{x}{a}\right)^2\right], \tag{28}$$

where $\Delta\Sigma_0$ is the magnitude of the electron density perturbation and a is its characteristic length. This yields

$$C(\Sigma) = a\sqrt{\ln\left(\frac{\Delta\Sigma_0}{\Sigma-\Sigma_0}\right)}. \tag{29}$$

According to Eq. (22), this distribution of the electron density corresponds to the following initial velocity distribution:

$$v|_{t=0} = 2s_0\left\{\sqrt{1+\frac{\Delta\Sigma_0}{\Sigma_0}\exp\left[-\left(\frac{x}{a}\right)^2\right]}-1\right\}. \tag{30}$$

If

$$\Sigma|_{t=0} = \Sigma_0 - \frac{2\Delta\Sigma_0}{\pi}\tan^{-1}\left(\frac{x}{a}\right), \tag{31}$$

one obtains

$$C(\Sigma) = a\tan\left[\frac{\pi}{2}\left(\frac{\Sigma_0-\Sigma}{\Delta\Sigma_0}\right)\right]. \tag{32}$$

Figures 2 and 3 show the transformation of the Riemann waves governed by Eq. (23), with the initial conditions given by Eqs. (28) and (31), respectively, up to the moments when conditions (26) and (27) are satisfied (up to $t=t_{br}$). These moments correspond to the rightmost curves in Figs. 2 and 3. The electron density and the coordinate in Figs. 2 and 3 are normalized by Σ_0 and s_0/ν, respectively. The obtained spatiotemporal variations of $\Sigma=\Sigma(t,x)$ and $v=v[\Sigma(t,x)]$ were compared with the results of direct numerical solution of Eqs. (14) and (15), and their coincidence was confirmed.

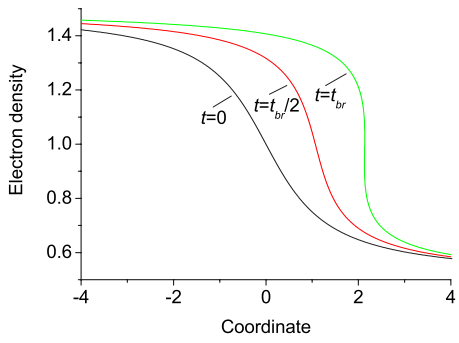

FIG. 3. (Color online) The same as in Fig. 2 but for the initial condition given by Eq. (31) and $\Delta\Sigma_0/\Sigma_0=0.5$.

The solutions obtained above are related to the formation of shock waves with zero front thickness. The inclusion of electron collisions and viscosity (that correspond to real systems) might affect the shape of the shock wave front. At a sufficiently sharp wave front, i.e., at a small thickness of the front δ, the viscosity term $-Kq^2v$ in Eq. (1) markedly exceeds the term associated with the electron collisions νv. Indeed, comparing these two terms and setting $q\sim\delta^{-1}$, one can find that the effect of viscosity dominates when $\delta<\sqrt{K/\nu}$. Using Eqs. (1), (12), and (13) (valid in the case of small gate layer thickness) and following the standard procedure,[35] the shock wave thickness determined by the viscosity can be estimated as $\delta\simeq K/s_0$. Substituting δ from this equation into the above inequality, we obtain the condition when the viscosity prevails the collisions in the formation of the shock wave front: $K\ll s_0^2/\nu=K_c$. Assuming $s_0=10^8$ cm/s and $\nu=10^{12}$ s^{-1}, we have $K_c\sim10^4$ cm^2/s. Since the characteristic value of the coefficient of viscosity in real 2DEG systems is $K\sim\hbar/m$ (see, for instance, Refs. 6 and 7), where $\hbar$ is the reduced Planck constant, for the GaAs channel, one obtains $K\sim15$ cm^2/s. This implies that $K\ll K_c$ and that the electron collisions should not affect the shape of the shock wave front as confirmed by the results on numerical modeling in the following.

In 2DEG systems where the gate layer is not too thin, the thickness of the wave front δ can be determined by the deviation of the plasma wave dispersion relation from the linear one (i.e., by 2D effects leading to a difference in the group velocities of the harmonics with different wave numbers q) rather than by the viscosity. Comparing the contributions of these two mechanisms, one can find that the first mechanism dominates if $K<s_0W_g=K_d$, with $K_d\simeq K_c(W_g\nu/s_0)$.

Thus, in 2DEG systems with a moderate gate layer thickness, the nonlinear waves should be fairly smooth, so that a solitonlike wave can form[26,27] rather than a shock wave. This is confirmed by the results of numerical simulations based on the general system of Eqs. (1)–(3) demonstrated in the next section.

IV. SHOCK AND SOLITONLIKE WAVES: NUMERICAL MODELING

Since an analysis of nonlinear regimes governed by the general equations of our model, which accounts for both the electron collisions and viscosity, i.e., Eqs. (1)–(3), cannot be realized analytically, we solved these equations numerically, considering for definiteness the upper structure in Fig. 1. The following dimensionless variables are used: time $\tau=t\nu$, coordinates $\xi=x\nu/s_0$ and $\eta=z\nu/s_0$, velocity $u=v/s_0$, electron density $\sigma=\Sigma/\Sigma_0$, and electric potential $\phi=e\varphi/ms_0^2$. In these

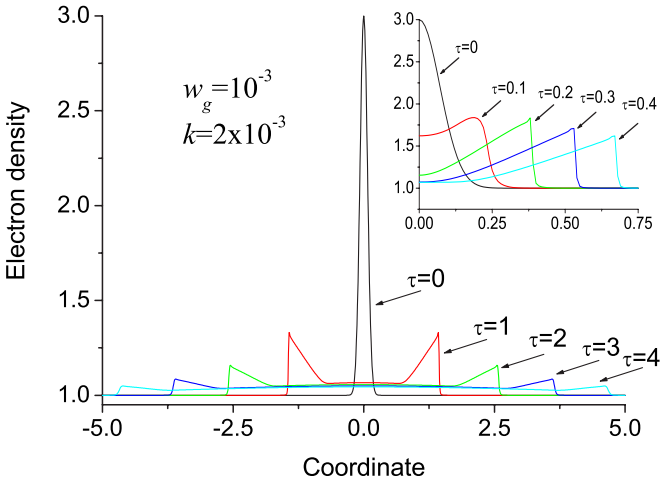

FIG. 4. (Color online) Evolution of spatial distributions of the normalized electron density Σ/Σ_0 in the 2DEG system with a normalized gate layer thickness $w_g=10^{-3}$. The inset corresponds to the early stage when the shock wave is formed. This case is analogous to the propagation of surface waves in a shallow water channel.

variables, the system of equations (1)–(3) is characterized by the following parameters: $\mathcal{L}_g=L_g\nu/s_0$, $w_g=W_g\nu/s_0=(W_g/L_g)\mathcal{L}_g$, $\tau_0=t_0\nu$, and $k=K\nu/s_0^2$. The Galerkin spectral method[38] was used in numerical calculations.

Figures 4–7 demonstrate the evolution of the spatial distributions of the electron density (normalized by Σ_0) in the structures with $\mathcal{L}_g=10$ and different normalized gate layer thicknesses ($w_g=0.001-1$) in response to a drastic change of the central gate section potential: $\Delta v_g=2\exp(-100\tau)$ ($\tau_0=10^{-2}$). It is assumed that $k=2\times10^{-3}$. These cases correspond to the spatial distributions of the electron density at the initial moment with a maximum at $x=0$, where $(\Sigma/\Sigma_d)|_{t=0}\simeq1.3-3$. If $s_0=10^8$ cm/s and $\nu=10^{12}$ s^{-1}, the results demonstrated in Figs. 4–7 correspond to the gate length $L_g=10$ μm (i.e., to a fairly long channel) and $W_g/L_g=10^{-4}-10^{-1}$. The length of the central gate section is about 0.5 μm. As shown, in systems with small values of the parameter w_g (Figs. 4 and 5), the initial perturbation of the electron density transforms into two pulses propagating from the channel center to the side contacts. After a short time, the front of these pulses becomes sharp, so the pulses turn into shock waves. In the case of small w_g and the pertinent conditions, our model, which includes the 2D Poisson equation, yields the same results as in papers by Dmitriev *et al.* [22] and Rudin and Samsonidze.[23,24] However, in 2DEG systems with larger values of the parameter w_g, the propagating waves have the form of relatively smooth pulses with a solitonlike shape (Fig. 6). At sufficiently large w_g, the transformation of the initial perturbation of the electron density (Fig. 7) is even qualitatively different from that in the case of effectively gated 2DEG systems. This difference in the nonlinear waves propagated in 2DEG systems with different parameters w_g can be attributed to a significant difference in the dispersion relations of the plasma waves in the cases of small and large spacings W_g (small and large values of parameter w_g).

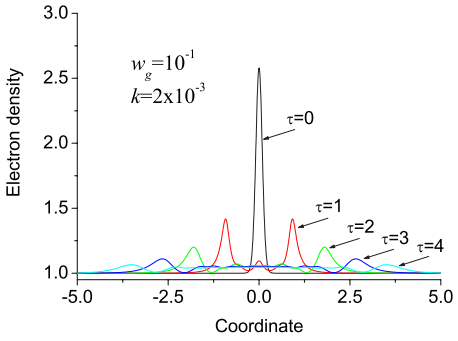

FIG. 6. (Color online) The same as in Fig. 4 but for $w_g=10^{-1}$.

As seen in Figs. 4–7, the amplitude of the propagating pulses markedly decreases with time. This effect is obviously associated with electron collisions. Comparing Figs. 4–6, one can see that the thickness of the wave front markedly increases with increasing w_g, characterizing the role of the plasma wave dispersion associated with the 2D nature of the distributions of the electrical potential in the systems under consideration.

Figure 8 shows the evolution of the electron density distributions in a 2DEG system with parameter k substantially smaller than in Figs. 4–7. One can see that in this case, the electron density distributions behind the shock wave front exhibit pronounced oscillations. To avoid numerical calculation artifacts, the pertinent modeling was conducted with rather different numbers of modes in the Fourier transformation (varied from 2×10^3 to 2×10^4). The independence of the result of the number of the modes used in the calculations was confirmed.

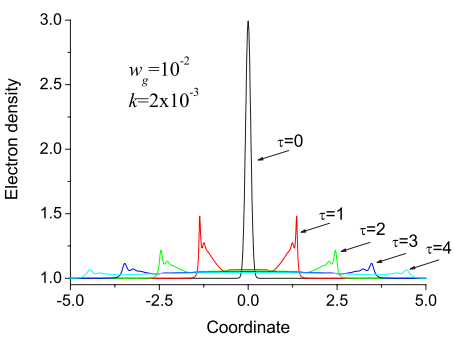

FIG. 5. (Color online) The same as in Fig. 4 but for $w_g=10^{-2}$.

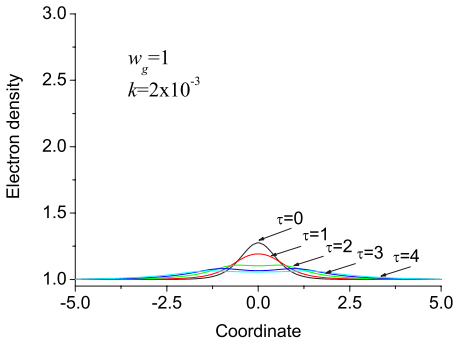

FIG. 7. (Color online) The same as in Fig. 4 but for $w_g=1$ (thick gate layer–deep water case).

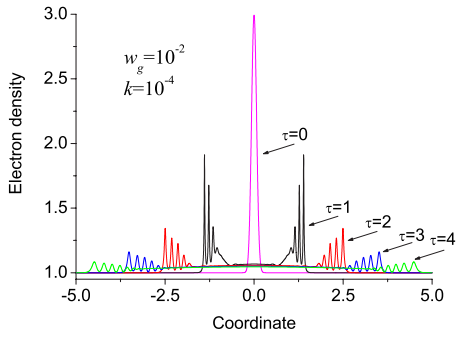

FIG. 8. (Color online) Snapshots of spatial distributions of the normalized electron density Σ/Σ_0 with an oscillatory structure behind the shock wave front in the system with a normalized gate layer thickness $w_g=10^{-2}$ and a small viscosity ($k=10^{-4}$).

The oscillatory character of the electron density distributions can be attributed to the instability of the shock waves with relatively smooth (but nonuniform) distributions behind the shock wave front. As shown previously,[39] the nonuniformity of 2DEG in the channel can markedly affect the conditions of plasma instability. Considering the nonuniformity of the electron density distribution in a propagating shock wave and assuming that the characteristic length of this perturbation q^{-1} is small in comparison with the scale of the nonuniformity of the electron density distribution behind the front, one can get the following equation for the damping rate of the electron density perturbations behind the front [compare with Eq. (10)]:

$$\mathrm{Im}\ \omega \simeq -\frac{1}{2}\left(\nu + Kq^2 - s_0\frac{d\ln\Sigma_0}{qdx}\right). \tag{33}$$

In the case $\mathrm{Im}\ \omega > 0$, i.e., when

$$\frac{d\ln\Sigma_0}{dx} > \frac{\nu + Kq^2}{s_0}, \tag{34}$$

the nonuniform but relatively smooth electron density distribution behind the shock wave front can become unstable, resulting in the formation of oscillatory distributions. This instability condition shows that the electron density distribution can be unstable when the gradient of the electron density is sufficiently large. Since the magnitude of the electron density peak decreases with wave propagation (due to electron collisions) and the total number of electrons is constant, the electron density gradient decreases as well. As a result, inequality (34) can be satisfied for the perturbations, with the spatial period increasing with time. Just such a behavior of the oscillatory structure behind the shock wave front is seen in Fig. 8.

Figure 9 shows how the velocity of the wave front (normalized by s_0) changes with time (normalized by ν^{-1}). We define the velocity of the wave front as the velocity of movement of the point where $\Sigma=(\Sigma_{max}+\Sigma_0)/2$. Here, Σ_{max} is the peak value of the electron density. One can see that in 2DEG systems with relatively thin gate layers, in which the formation of the shock waves occurs (corresponding to Figs. 4 and 5), the velocity of the front movement exceeds the characteristic plasma wave velocity s_0, but this front movement decelerates with elapsed time. This can be attributed to the fact that according to the general properties of shock waves[34] (see also Ref. 24), their velocity is determined by s_0 and $s=s_0\sqrt{\Sigma/\Sigma_0}$ [see Eq. (20)], with the latter value decreasing throughout the wave propagation (as seen in Figs. 4 and 5). However, the velocity of propagation of more smooth pulses (see curve marked by squares in Fig. 9) in the case of larger gate thicknesses is close to s_0.

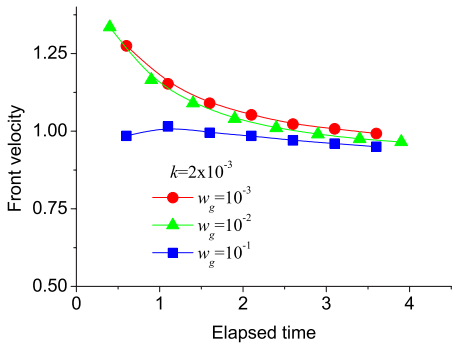

FIG. 9. (Color online) Time dependences of the front velocity for the same parameters as in Figs. 4–6.

The results shown in Figs. 4–8 correspond to a relatively fast switch-off of the voltage applied to the central gate section ($\tau_0=10^{-2}$). The obtained results do not change when τ_0 increases up to $\tau_0=10^{-1}$. However, at relatively slow voltage switch-off, i.e., at moderate values of parameter τ_0, the pattern of relaxation of electron density becomes markedly different. Figure 10 shows the relaxation of electron density in the 2DEG system with the same parameters as in Fig. 4 at $\tau_0=1$. In this case, the transformation of the electron density distribution closely resembles the density peak smearing considered previously in the framework of the conductive model.[22,40]

V. WAVE PROPAGATION IN NONUNIFORM CHANNEL: EFFECT OF "TSUNAMI"

Consider now a 2DEG system with markedly nonuniform distribution of donors $\Sigma_d=\Sigma_d(x)$ along the channel, so that the quantity Σ_0 given by Eq. (7) also depends on the coordinate x. We assume that

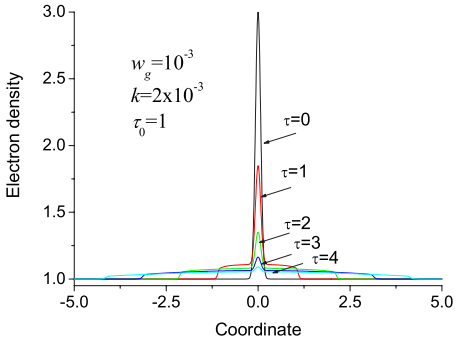

FIG. 10. (Color online) Evolution of the spatial distribution of the normalized electron density Σ/Σ_0 in the 2DEG system with the same parameters as in Fig. 4 but at a relatively slow voltage switch-off ($\tau_0=1$).

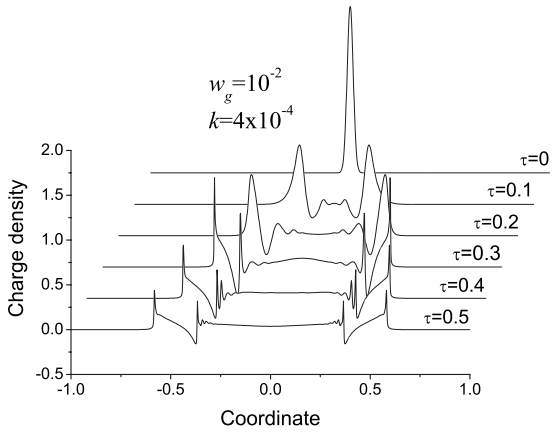

FIG. 11. Evolution of the spatial distribution of the normalized sheet charge $(\Sigma-\Sigma_0)/\langle\Sigma_0\rangle$ in the 2DEG system with a nonuniform donor distribution.

$$\Sigma_d = \begin{cases} \Sigma_d^c & \text{if } |x| < L_0, \\ \Sigma_d^e + (\Sigma_d^c - \Sigma_d^e)e^{-(2|x| - L_d/2a_d)^2} & \text{if } |x| > L_0, \end{cases}$$

where Σ_d^c is the sheet density of donors in the channel center, Σ_d^e is the donor density near its edges, and L_d and a_d are the characteristic lengths of the spatial distribution of donors $(L_d < L)$. Figure 11 shows the evolution of the spatial distribution of the sheet charge density in the 2DEG channel normalized by $\langle\Sigma_0\rangle$, where the symbol $\langle\cdots\rangle$ means the averaging over the channel length. One can see that two solitonlike waves propagating in opposite directions toward the side contacts arise. However, upon reaching the regions with a relatively low donor density $(\tau\sim 0.25)$, these waves transform into shock waves with rather sharp fronts and complex structures behind the front. In particular, the fronts are followed by depletion regions and then by the secondary shock waves. The behavior pattern of the wave that originated from the initial pulse resembles a tsunami in the ocean. This is due to an analogy between the equations governing the 2DEG in the systems under consideration and the equations describing the gravity surface waves in shallow and deep water pools.

VI. CONCLUSIONS

We studied the electrical excitation of nonlinear plasma waves in heterostructures with 2DEG channels and split gates. The propagation of these waves was considered both analytically and using numerical modeling. The hydrodynamic electron transport model accounted for electron collisions with impurities and phonons as well as 2DEG viscosity. The hydrodynamic equations were supplemented by the 2D Poisson equation for the self-consistent electric potential. We demonstrated the formation of shock and solitonlike waves as a result of the evolution of strongly nonuniform initial electron density distribution. It was found that the shock wave front and the shape of solitonlike pulses pronouncedly depend on the coefficient of 2DEG viscosity, the thickness of the gate layer, and the nonuniformity of the donor distribution along the channel. In the case of the 2DEG channel with a strongly nonuniform doping, the effect of transformation of relatively smooth waves into shock waves, resembling a tsunami effect, was observed. The electron collisions result in the damping of the shock and solitonlike waves. However, they do not markedly affect the thickness of the shock wave front. Due to the fairly sharp wave front of nonlinear waves in the 2DEG systems under consideration or due to their strongly oscillatory structure (as shown in Fig. 8), the transient charges induced by the propagating charges of these waves in the side contacts and, hence, in the external circuit might exhibit steep surges. Fast transient currents in such a circuit including an antenna might provide generation of electromagnetic radiation with relatively high frequencies. The heterostructures with a nonuniform doping of 2DEG channel appears to be rather promising. In the structures with the gate separated into several short sections (see the lower structure in Fig. 1), the propagating charges of shock waves might result in even steeper surges of the charges induced in these sections.[41] Since these sections can serve as antenna components, fast variations of the induced charges and, hence, the dipole momentum can lead to the emission of electromagnetic radiation. There are several characteristic frequencies related to the situation: $f_1 \sim s_0/L_g$, $f_2 \sim s_0/l_g$, where l_g is the lateral spacing between the neighboring gate sections, and $f_3 \sim s_0/\delta$. The frequencies f_1, f_2, and f_3 can be much larger that the inverse recharging time t_0^{-1} easily falls in the terahertz range at realistic values of the characteristic lengths due to fairly large values of the characteristic velocity of plasma wave s_0 (about 10^8 cm/s). The mechanism of the generation of relatively high frequency electrical signals, which convert into electromagnetic radiation, is akin to the frequency multiplication due to the plasma nonlinearity. Thus, the excitation of shock and solitonlike waves in the heterostructures under consideration by external electrical signals might be used to generate terahertz radiation.

ACKNOWLEDGMENTS

The authors are grateful to R. Gupta and A. Satou for comments on the manuscript. One of the authors (V.R.) thanks T. Otsuji, A. Chaplik, and M. S. Shur for stimulating discussions. This work was supported by the Grant-in-Aid for Scientific Research (S) from the Japan Society for Promotion of Science, Japan.

*v-ryzhii@u-aizu.ac.jp

[1] F. Stern, Phys. Rev. Lett. **18**, 546 (1967).
[2] A. V. Chaplik, Sov. Phys. JETP **35**, 395398 (1972).
[3] N. Nakayama, J. Phys. Soc. Jpn. **36**, 393 (1967).
[4] S. J. Allen, Jr., D. C. Tsui, and R. A. Logan, Phys. Rev. Lett. **38**, 980 (1977).
[5] D. Heitmann, Surf. Sci. **170**, 332 (1986).
[6] M. Dyakonov and M. Shur, Phys. Rev. Lett. **71**, 2465 (1993).
[7] M. Dyakonov and M. S. Shur, IEEE Trans. Electron Devices **43**, 1640 (1996).
[8] M. S. Shur and V. Ryzhii, Int. J. High Speed Electron. Syst. **13**, 575 (2003).
[9] X. G. Peralta, S. J. Allen, M. C. Wanke, N. E. Harff, J. A. Simmons, M. P. Lilly, J. L. Reno, P. J. Burke, and J. P. Eisenstein, Appl. Phys. Lett. **81**, 1627 (2002).
[10] N. Sekine, K. Hirakawa, M. Voßebürger, P. H. Bolivar, and H. Kurz, Phys. Rev. B **64**, 201323(R) (2001).
[11] Y. Deng, R. Kersting, J. Xu, R. Ascazubi, X.-C. Zhang, M. S. Shur, R. Gaska, G. S. Simin, M. Asif Khan, and V. Ryzhii, Appl. Phys. Lett. **84**, 70 (2004).
[12] W. Knap, J. Lusakowski, T. Parently, S. Bollaert, A. Cappy, V. V. Popov, and M. S. Shur, Appl. Phys. Lett. **84**, 2331 (2004).
[13] J. Lusakowski, W. Knap, N. Dyakonova, L. Varani, J. Mateos, T. Gonzales, Y. Roelens, S. Bullaert, A. Cappy, and K. Karpierz, J. Appl. Phys. **97**, 064307 (2005).
[14] F. Teppe, D. Veksler, V. Yu. Kacharovskii, A. P. Dmitriev, S. Rumyantsev, W. Knap, and M. S. Shur, Appl. Phys. Lett. **97**, 022102 (2005).
[15] T. Otsuji, M. Hanabe, and O. Ogawara, Appl. Phys. Lett. **85**, 2119 (2004).
[16] M. Hanabe, T. Otsuji, T. Ishibashi, T. Uno, and V. Ryzhii, Jpn. J. Appl. Phys., Part 1 **44**, 3842 (2005).
[17] N. Sekine, K. Yamanaka, K. Hirakawa, M. Vosseburger, P. Haring Bolivar, and H. Kurz, Appl. Phys. Lett. **74**, 1006 (1999).
[18] I. V. Kukushkin, J. H. Smet, V. A. Kovalskii, S. I. Gubarev, K. von Klitzing, and W. Wegscheider, Phys. Rev. B **72**, 161317(R) (2005).
[19] I. V. Kukushkin, V. M. Muravev, J. H. Smet, M. Hauser, W. Dietsche, and K. von Klitzing, Phys. Rev. B **73**, 113310 (2006).
[20] V. A. Kovalskii, S. I. Gubarev, I. V. Kukushkin, S. A. Mikhailov, J. H. Smet, K. von Klitzing, and W. Wegscheider, Phys. Rev. B **73**, 195302 (2006).
[21] M. I. Dyakonov and A. S. Furman, Sov. Phys. JETP **65**, 574 (1987).
[22] A. P. Dmitriev, A. S. Furman, V. Yu. Kachorovskii, G. G. Samsonidze, and Ge. G. Samsonidze, Phys. Rev. B **55**, 10319 (1997).
[23] S. Rudin and G. Samsonidze, Phys. Rev. B **58**, 16369 (1998).
[24] S. Rudin, G. Samsonidze, and F. Crowne, J. Appl. Phys. **86**, 2083 (1999).
[25] M. V. Cheremisin, Phys. Rev. B **65**, 085301 (2002).
[26] A. Nerses and E. E. Kunhard, J. Math. Phys. **39**, 6392 (1998).
[27] A. O. Govorov, V. M. Kovalev, and A. V. Chaplik, JETP Lett. **70**, 488 (1999).
[28] V. Ryzhii, Jpn. J. Appl. Phys., Part 1 **37**, 5937 (1998).
[29] V. Ryzhii and M. S. Shur, Jpn. J. Appl. Phys., Part 1 **40**, 546 (2001).
[30] V. Ryzhii and M. S. Shur, Jpn. J. Appl. Phys., Part 2 **45**, L1118 (2006).
[31] A. Satou, I. Khmyrova, A. Chaplik, V. Ryzhii, and M. S. Shur, Jpn. J. Appl. Phys., Part 1 **44**, 2592 (2005).
[32] M. Dyakonov and M. S. Shur, Appl. Phys. Lett. **87**, 111501 (2005).
[33] A. Satou, V. Ryzhii, and A. Chaplik, J. Appl. Phys. **98**, 034502 (2005).
[34] V. Ryzhii, A. Satou, W. Knap, and M. S. Shur, J. Appl. Phys. **99**, 084507 (2006).
[35] L. D. Landau and E. M. Lifshitz, *Fluid Mechanics* (Butterworth-Heinemann, Oxford, 2003).
[36] R. Sagdeev, in *Reviews of Plasma Physics*, edited by M. A. Leontovich (Consultant Bureau, New York, 1964).
[37] A. A. Ivanov, *Physics of Strongly Non-Equilibrium Plasmas* (Atomisdat, Moscow, 1977) (in Russian).
[38] C. A. J. Fletcher, *Computational Techniques for Fluid Dynamics* (Springer, New York, 1988).
[39] M. V. Cheremisin and G. G. Samsonidze, Semiconductors **33**, 578 (1999).
[40] A. Y. Shik, Semiconductors **29**, 697 (1995).
[41] Numerical calculations, using the above model and the Shockley-Ramo theorem, of the displacement currents through the gate sections in the lower structure in Fig. 1 induced by propagating shock waves show that the current pulses have a triangular shape with a rather short rise (with the characteristic time l_g/s_0) and relatively slow (with the characteristic time L_g/s_0) decay. I. Semenikhin, V. Ryzhii, E. Vostrikova, and A. Ivanov (unpublished).